

Supplemental Information

**Divergent synaptic dynamics originate
parallel pathways for computation
and behavior in an olfactory circuit**

Hyong S. Kim, Gustavo Madeira Santana, Gizem Sancer, Thierry Emonet, and James M. Jeanne

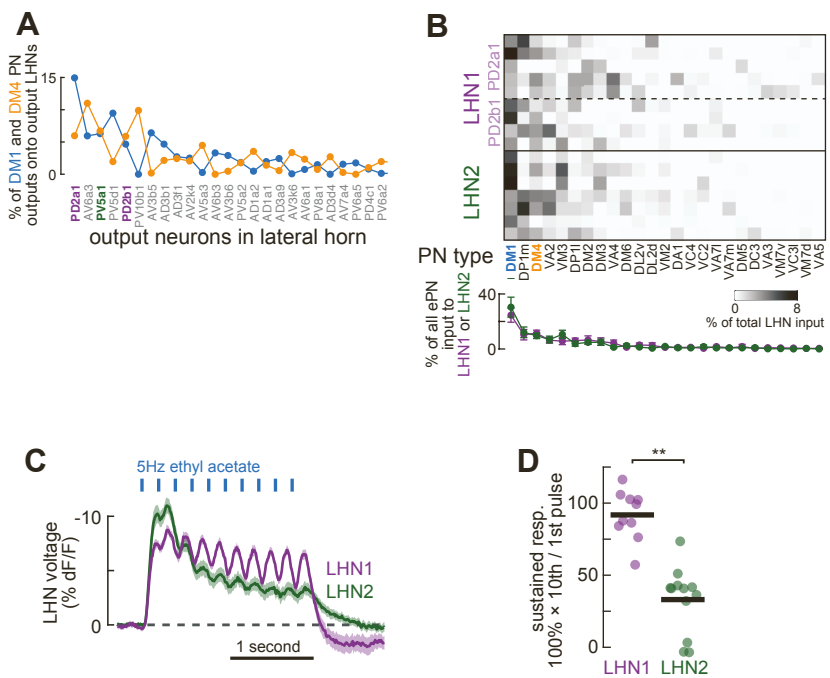


Figure S1: LHN connectivity and voltage imaging. Related to Figure 1.

(A) Average distribution of synapses onto output LHN types from the DM1 and DM4 PNs (as a fraction of all synapses from each PN that target output LHNs). Data from Hemibrain connectome.

(B) Top: input to each instance of LHN1 and LHN2, for the top 25 cholinergic uniglomerular PN inputs (as a fraction of all input to each LHN). Bottom: average distribution of synapses onto LHN1 and LHN2 types from the top 25 cholinergic uniglomerular PNs (as a fraction of all cholinergic uniglomerular inputs per LHN type).

(C) Mean (\pm s.e.m.) voltage change (ArcLight fluorescence) of LHN1 ($n = 10$) and LHN2 ($n = 12$) in response to 5Hz ethyl acetate odor stimulus. Voltage scale is inverted because fluorescence decreases with voltage.

(D) Comparison of sustained responsiveness (10th pulse amplitude as a percentage of 1st pulse amplitude) in LHN1 and LHN2. T test: ** $p < 0.001$.

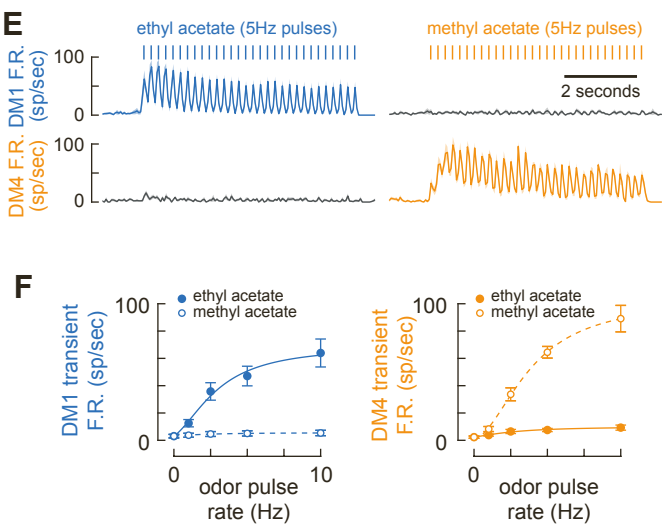
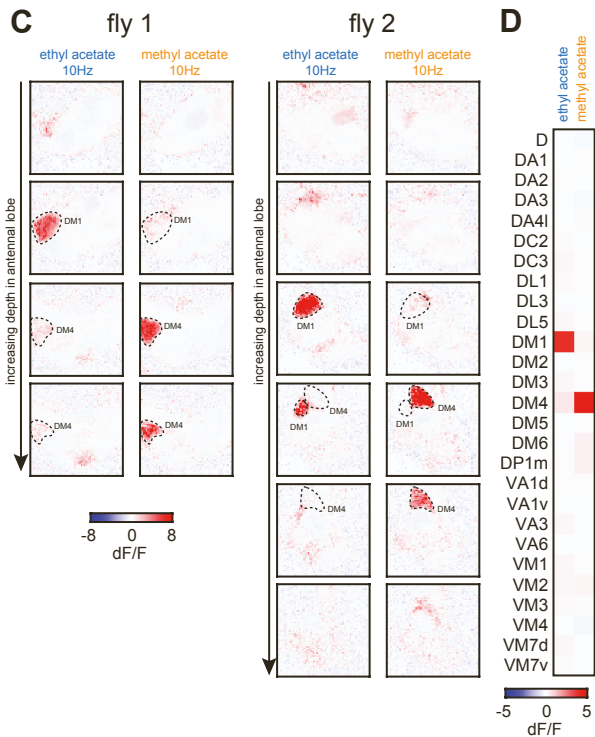
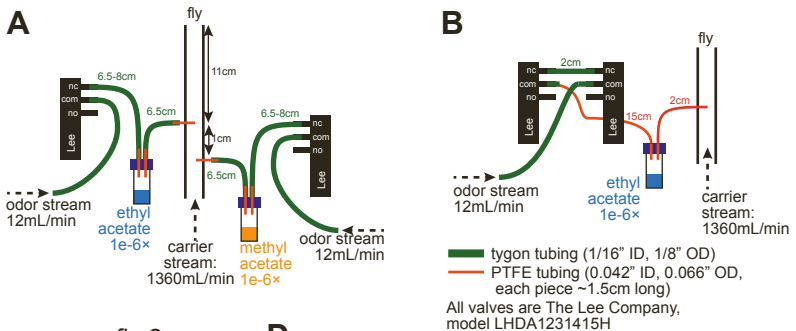


Figure S2. Odor delivery and validation of private odor stimulation. Related to Figure 1.

(A) Schematic of odor delivery device used for all experiments except for those in Figure 6A,B.

(B) Schematic of odor delivery device used for experiments in Figure 6A,B. This design used an extra valve so that the headspace in the odor vial was always vented away from the carrier stream. This was designed for the use of higher concentration odors to prevent odor leaking into the carrier stream. However, none of the odors used in this study were high enough concentration to cause leakage. The only functional difference between the designs in (A) and (B) is that (B) has a longer latency for odor to reach the fly. Thus, for the data reported in Figure 6A,B, valves were opened for 150msec instead of 40msec. nc = normally closed. no = normally open. com = common.

(C) 2-photon calcium imaging of GH146-Gal4 / UAS-GCaMP6f in several planes in the antennal lobe in 2 different flies, in response to 10Hz ethyl acetate or 10Hz methyl acetate (the highest intensity odors used for physiology). Ethyl acetate is specific for DM1 and methyl acetate is specific for DM4, as seen with electrophysiology. No substantial calcium response in any other glomerulus is observed, indicating that our stimuli are private, consistent with previous studies that have used these odors.

(D) Average GCaMP fluorescence amplitude for PNs in each specified glomerulus.

(E) Mean (\pm s.e.m.) PSTHs of DM1 (top, n = 8) and DM4 (bottom, n = 5) spike rates in response to 5Hz ethyl acetate (left) and 5Hz methyl acetate (right). Spike rates are determined from whole-cell patch clamp electrophysiology.

(F) Tuning curves of initial transient spike rates (mean \pm s.e.m., computed within the first 1 second of response) for ethyl and methyl acetate in DM1 (n = 8) and in DM4 (n = 5). The lack of substantial responses for the off-target odor in each PN type further validates the privacy of these odor stimuli.

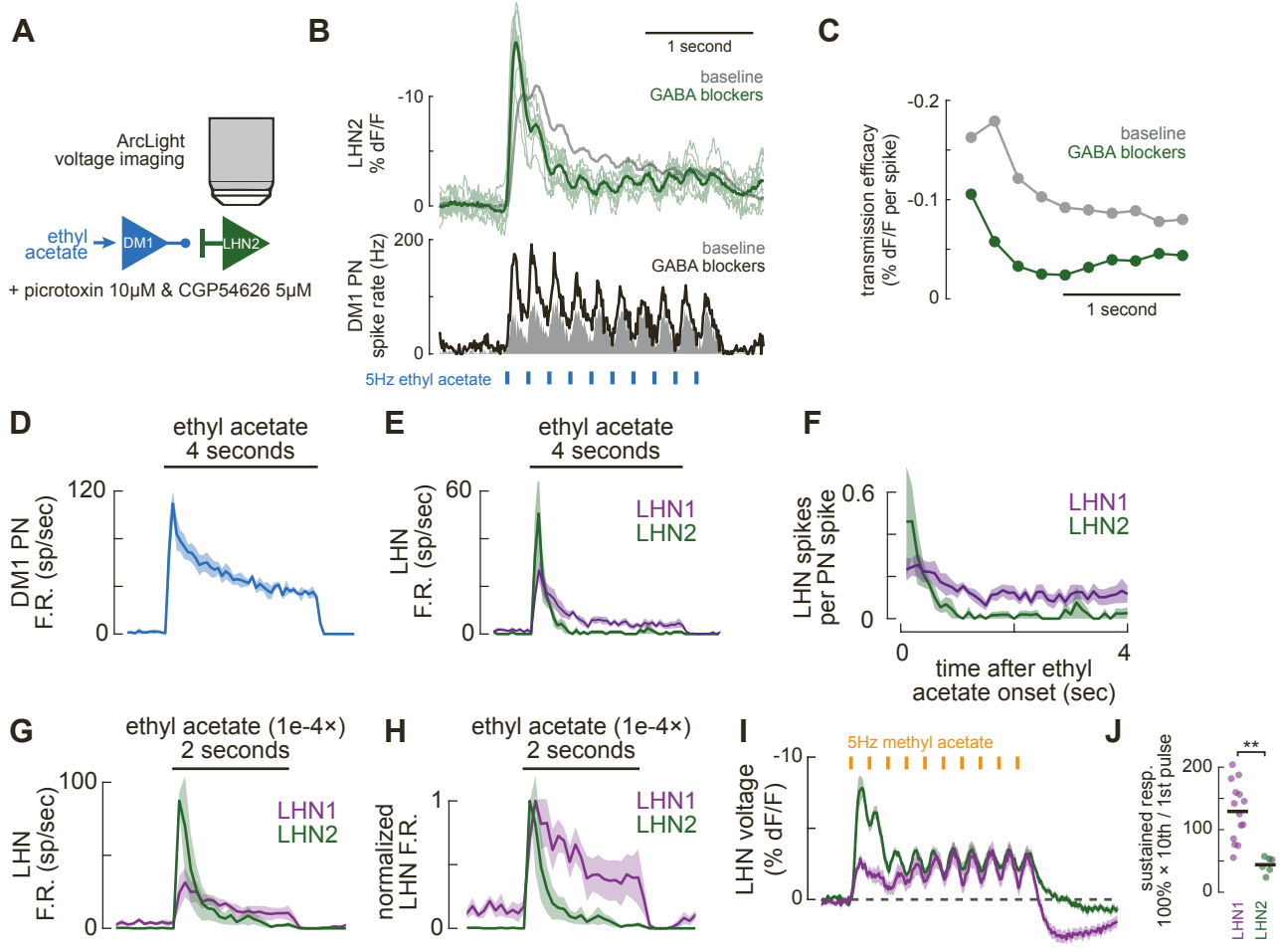


Figure S3. LHN2 adaptation does not require synaptic inhibition and broad differences in LHN dynamics are not stimulus specific. Related to Figure 1.

- (A)** Schematic of experimental test of the role of synaptic inhibition in LHN2 dynamics. In each experiment, baseline odor responses were recorded, picrotoxin and CGP54626 were bath-applied to block GABA-A and GABA-B receptors, and then odor responses were recorded again. Because bath application also affects PN responses to odors, we also measured PN spike rates during identical pharmacological manipulation.
- (B)** Top: comparison of responses to 5Hz ethyl acetate in LHN2 before and after pharmacological blockade of GABA receptors. With blockers, adaptation to odor pulses becomes slightly stronger (thin green lines are single recordings, thick green line is the mean) than the mean response in control saline (gray). Bottom: GABA blockers also increase DM1 PN adaptation, mostly by increasing responses to the first few odor pulses.
- (C)** Voltage responses per odor pulse in LHN2 normalized by the number of DM1 spikes per pulse. Each point is the mean response to each odor pulse. Blocking GABAergic inhibition does not dramatically change the adapting dynamics of the “transmission efficacy” relating PN spikes to LHN voltage.
- (D)** Mean (\pm s.e.m.) PSTHs of DM1 ($n = 3$) in response a 4-second solid pulse of ethyl acetate (at 1×10^{-6} concentration), showing that responses are sustained, but adapt modestly, similar to pulsed odor stimulation.
- (E)** Mean (\pm s.e.m.) PSTHs of LHN1 ($n = 8$) and LHN2 ($n = 3$) in response to the same 4-second solid pulse of ethyl acetate as in panel D, showing sustained activity in LHN1, but not in LHN2, similar to pulsed odor stimulation.
- (F)** Mean (\pm s.e.m.) LHN spikes per PN spike during the same 4-second solid pulse of ethyl acetate (data from panels D,E). Responses are binned into 100msec bins. Both LHN types adapt, but LHN2 adapts more strongly than LHN1, similar to our main observations with pulsed stimuli.
- (G)** Mean (\pm s.e.m.) PSTHs of LHN1 ($n = 4$) and LHN2 ($n = 3$) responses to a 2-second solid pulse of ethyl acetate at 1×10^{-4} concentration, which activates multiple glomeruli, including DM1 and DM4.
- (H)** Same as (D), but with PSTHs normalized by their peak value.
- (I)** Mean (\pm s.e.m.) voltage change (ArcLight fluorescence) of LHN1 ($n = 10$) and LHN2 ($n = 12$) in response to 5Hz pulses of methyl acetate (at 1×10^{-6} concentration, which privately activates the DM4 glomerulus; Figure S2). Voltage scale is inverted because fluorescence decreases with voltage increases.
- (J)** ArcLight responses to methyl acetate persist more in LHN1 than in LHN2 (similar to responses to ethyl acetate). T tests: ** $p < 0.001$.

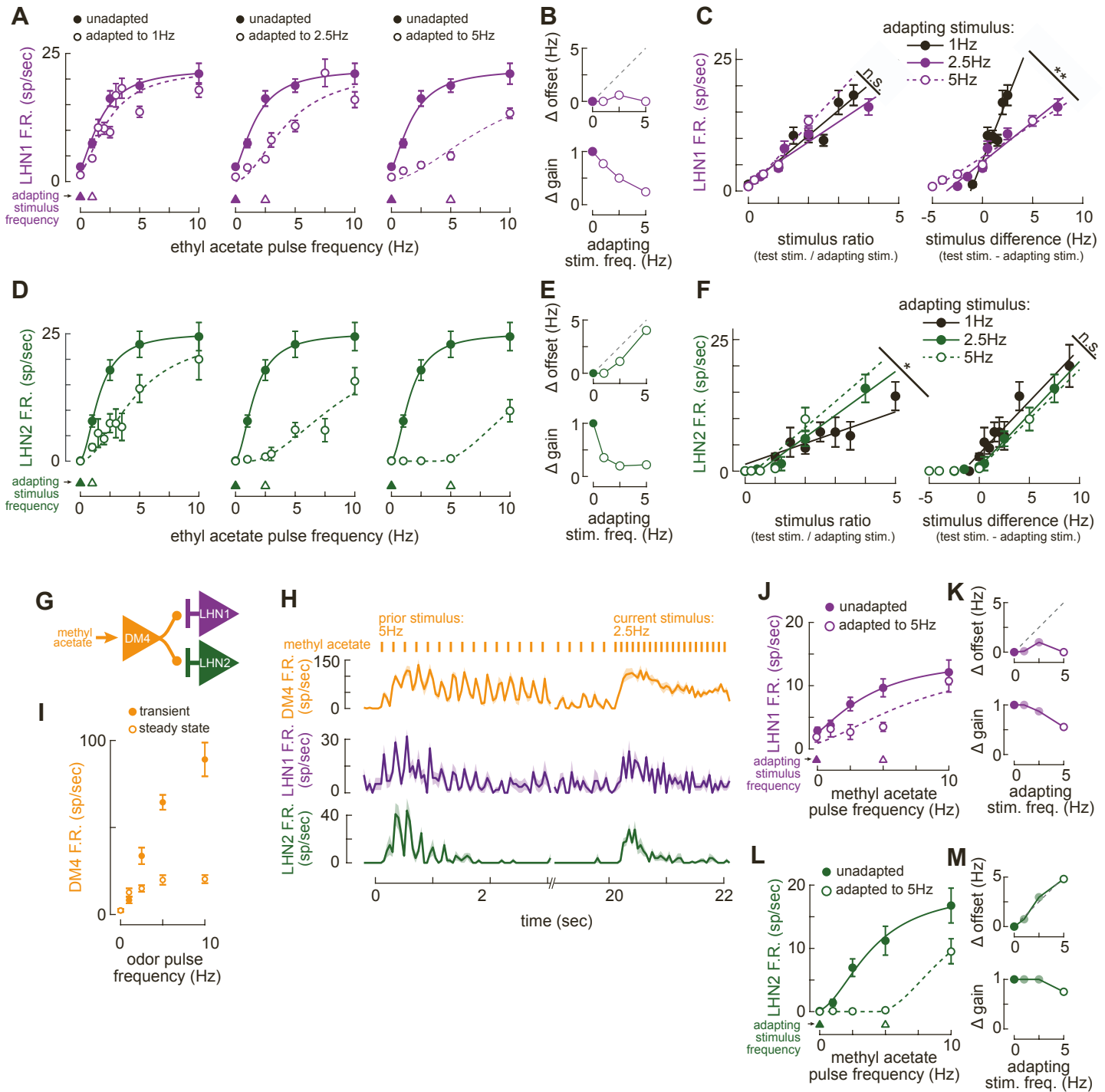


Figure S4. Adaptation to different frequencies and odors. Related to Figure 1.

(A) Mean (\pm s.e.m.) ethyl acetate responses for LHN1 ($n = 9-16$) for a range of stimulus frequencies without adaptation (solid circles) and with adaptation (open circles) to 1Hz (left) 2.5Hz (middle) and 5Hz (right). Solid curves are fit to unadapted spike rates, and then only its offset and gain were adjusted to fit the adapted data (dashed curve; **STAR Methods**). Adapting pulse frequencies are plotted in triangles at bottom.

(B) Change in offset (top) and gain (bottom) for the best fit curves to LHN1 responses to each adaptation frequency.

(C) LHN1 spike rates as a function of stimulus ratio (left) or stimulus difference (right). Only the linear regimes of responses from panel A are included. Best linear fits for each adapting frequency have indistinguishable slopes for stimulus ratio but not stimulus difference, indicating that LHN1 encodes stimulus ratio better than difference. ** ANCOVA interaction, $p = 0.005$.

(D) Same as (A) but for LHN2 ($n = 6-16$).

(E) Same as (B) but for LHN2.

(F) Same as (D) but for LHN2, which encodes stimulus difference better than ratio. ** ANCOVA interaction, $p = 0.011$.

(G) Schematic of divergence from the DM4 PN onto LHN1 and LHN2.

(H) Mean (\pm s.e.m.) PSTHs of DM4 (top, $n = 5$), LHN1 (middle, $n = 6$), and LHN2 (bottom, $n = 5$) in response 20 seconds of 5Hz pulses of methyl acetate, which is then switched to 10Hz.

(I) Comparison of transient and steady state spike rates of DM4 in response to methyl acetate stimulation at a range of pulse rates.

(J) Tuning curves for mean (\pm s.e.m.) LHN1 ($n = 6-16$) spike rates to a range of methyl acetate pulse frequencies without adaptation (solid circles) and after adaptation to a prior frequency of 5Hz methyl acetate (open circles). Curves are fit with the same procedure and model as for ethyl acetate stimulation (**STAR Methods**).

(K) Change in offset (top) and gain (bottom) for the best fit curves to LHN1 responses to each adaptation frequency.

(L) Same as (J) but for LHN2 ($n = 5-12$).

(M) Same as (K) but for LHN2.

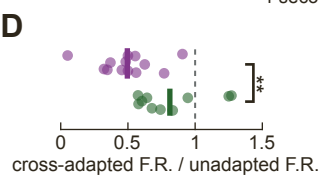
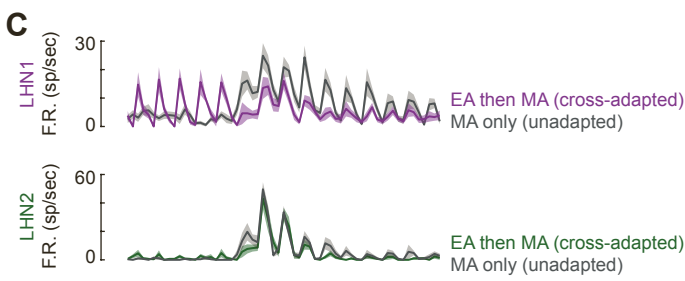
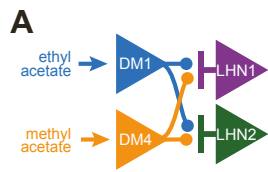


Figure S5. Adaptation in LHN2 is more input-specific than adaptation in LHN1. Related to Figures 1 and 2

(A) Schematic showing the connectivity of DM1, DM4, LHN1, and LHN2 underlying the cross-adaptation experiment. Both DM1 and DM4 diverge onto LHN1 and LHN2.

(B) Top: mean (\pm s.e.m.) responses of DM4 PNs ($n = 3$) to 5Hz ethyl acetate then 5Hz methyl acetate (orange) or to methyl acetate alone (gray). Bottom: mean (\pm s.e.m.) responses DM1 PNs ($n = 4$) to ethyl acetate then methyl acetate (blue) or to methyl acetate alone (gray). No evidence of cross adaptation is apparent in either PN type. These plots, and those in (C), only show the end of ethyl acetate stimulation, which had fully adapted by the time the odor switched to methyl acetate.

(C) Top: mean (\pm s.e.m.) responses of LHN1 ($n = 13$) to 5Hz ethyl acetate then 5Hz methyl acetate (purple) or to methyl acetate alone (gray). Bottom: mean (\pm s.e.m.) responses of LHN2 ($n = 10$) to 5Hz ethyl acetate then 5Hz methyl acetate (green) or to methyl acetate alone (gray).

(D) Normalized cross-adapted responses (cross-adapted F.R. / unadapted F.R.) are smaller in LHN1 than in LHN2 (** t-test, $p = 0.0043$), indicating greater cross-adaptation in LHN1.

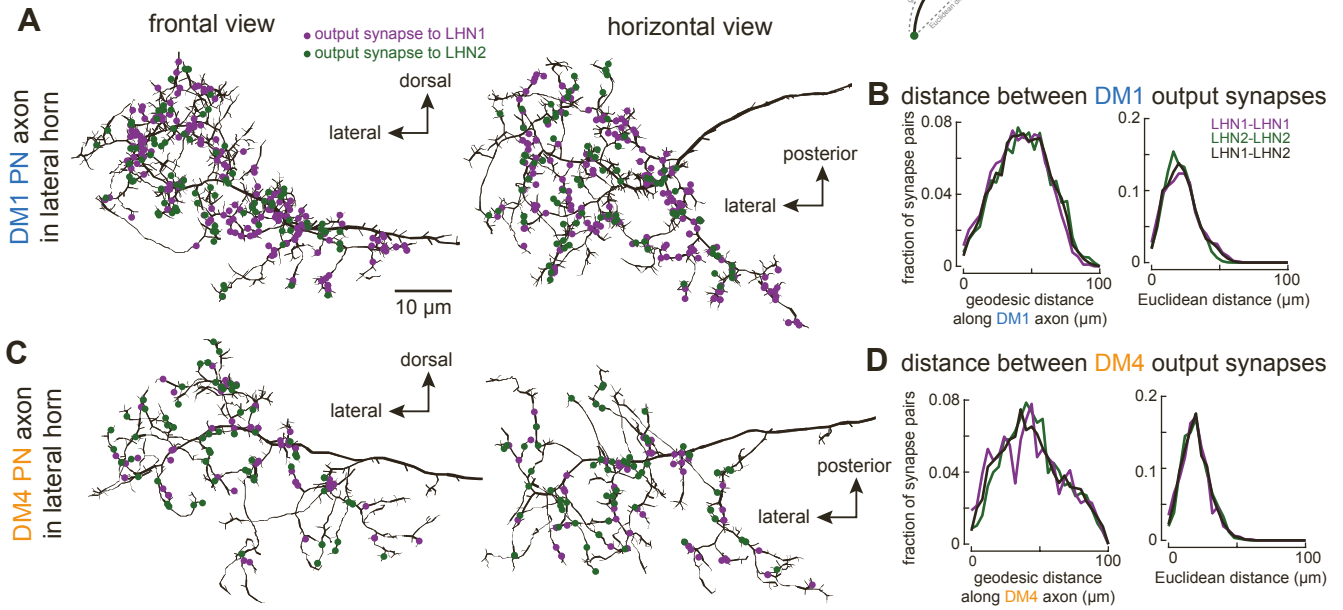


Figure S6. PN synapses onto LHN1 and LHN2 are not spatially organized. Related to Figures 3 and 4.

(A) Synapse locations on the DM1 PN axon in the lateral horn onto LHN1 (purple) and LHN2 (green). Frontal and horizontal are two different views of the same axon. There is no obvious spatial or branch-specific organization to synapse locations.

(B) Distributions of geodesic (left) and Euclidean (right) distances between every pair of LHN1 and LHN2 synapses on the DM1 axon in the lateral horn. Geodesic distance is the distance along the neurite (see schematic above). There are no substantial differences between these distributions.

(C,D) Same as (A,B) but for the DM4 axon.

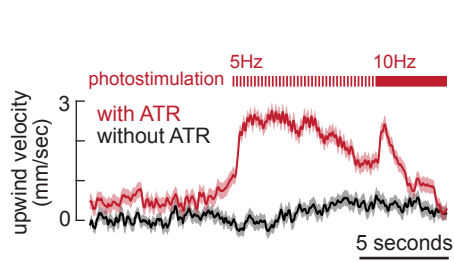
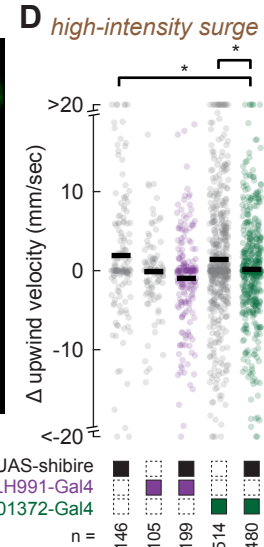
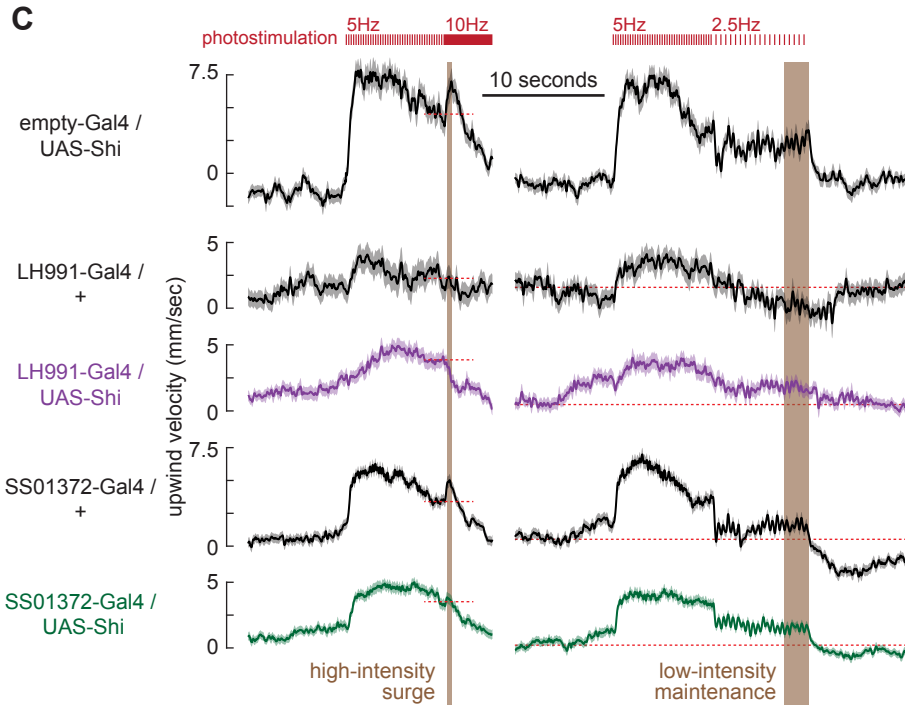
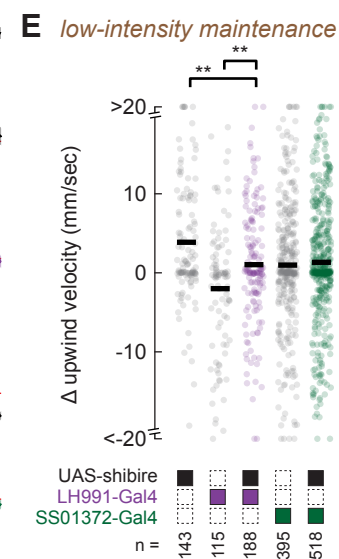
A**B****D****C****E**

Figure S7. Additional behavioral controls and genotypes for genetic silencing. Related to Figure 7.

(A) Red light-evoked upwind walking is due to optogenetic activation of DM1 ORNs, and not direct activation of the visual system (or any other effect of red light). CsChrimson requires all-*trans* retinal (ATR) in the diet to function properly. Omitting it abolishes nearly all light-evoked upwind walking. Traces are the mean (\pm s.e.m.) upwind velocity traces of Or42b-LexA, LexAop-CsChrimson ; SS01372-Gal4/+ flies with (red) or without (black) ATR.

(B) Expression patterns of the additional Gal4 lines used to silence each LHN type. LH991-Gal4 targets LHN1 and SS01372-Gal4 targets LHN2. Some off-target expression is evident in each line but is different from that in the corresponding Gal4 lines used in Figure 7. Note that LH991-Gal4 also labels an additional LHN type.

(C) Mean (\pm s.e.m.) upwind velocity traces of flies in each genotype to 5Hz to 10Hz photostimulation and 5Hz to 2.5Hz photostimulation patterns. Data for genotypes that silence LHN1 and LHN2 are displayed in purple and green, respectively. Parental control genotypes are displayed in black. Gray background shading denotes time windows for analysis of the high-intensity surge and low-intensity maintenance analyzed in (D,E). Red dotted lines indicate walking speeds just prior to the 10Hz stimulus (left) or in the absence of stimulus (right), from which the values in (D,E) are calculated.

(D) Summary of the magnitude of the high intensity surge for all flies in each genotype. Each point denotes one fly trajectory, sample sizes specified at the bottom denote number of trajectories. T-tests: * $p < 0.02$.

(E) Same as (C) but for the magnitude of the low intensity maintenance. T-tests: ** $p < 0.005$.

Flies expressing LH991-Gal4 (either with or without UAS-Shibire) had an unusually strong attraction to the walls of the arena, where they walked very little, meaning that many of these flies did not respond to fictive odor stimulation. Furthermore, flies of the parental control genotype LH991-Gal4/+ that did respond to light exhibited unusually small increases in upwind velocity, without an upwind surge to the onset of 10Hz stimulation (the upwind surge was observed in every other control genotype we tested). The experiment of silencing LH991-expressing neurons was therefore inconclusive. We note that LH989-Gal4 has off-target expression in only a few neurons in the ventral nerve cord. While silencing those neurons could affect walking, they would be expected to disrupt walking more broadly, and not in a manner that is selective for specific fictive odor frequencies. It is thus most likely that driving *shibire* with LH989-Gal4 impacts behavior by disrupting LHN1 rather than the neurons in the ventral nerve cord.